



## SEISMIC PERFORMANCE OF POLYPROPYLENE FIBER-REINFORCED CONCRETE COLUMN WITH CORRODED REINFORCING BARS

A. Aryanto <sup>(1)</sup> and B.J. Winata <sup>(2)</sup>

<sup>(1)</sup> Assistant Professor, Structural Engineering Research Group, Faculty of Civil and Environmental Engineering, Institut Teknologi Bandung, Indonesia, [arisaryanto@ftsl.itb.ac.id](mailto:arisaryanto@ftsl.itb.ac.id)

<sup>(2)</sup> Research Student, Structural Engineering Research Group, Faculty of Civil and Environmental Engineering, Institut Teknologi Bandung, Indonesia, [Berto.juergen@hotmail.com](mailto:Berto.juergen@hotmail.com)

### Abstract

Specific guidelines on design or assessment of the seismic performance of existing polypropylene fiber reinforced concrete (PPFRC) structures, especially suffered from corrosion, are still not available. Consequently, this may lead to unsafe consideration when the seismic evaluation is conducted on such structures. From previous research, fibers in the reinforced concrete are known to improve the seismic performance, in reverse corrosion adversely affect the reinforced concrete performance. In this study, the combined effect of both fiber addition and corrosion on RC structures behaviors are evaluated. Experimental work has been conducted to study the effect of reinforcing bars corrosion on the seismic performance of PPFRC columns. Five columns, including polypropylene fiber addition, were subjected to different levels of corrosion from slight to severe using an impressed current imposed to steel reinforcement and then were tested under reversed cyclic lateral loading. The seismic performance of columns was assessed in terms of lateral load, crack pattern, hysteretic response, drift capacity, and energy dissipation capacity. The results proved that the fiber addition improves lateral load, drift, and energy dissipation capacity of columns. Meanwhile, corroded columns suffered degradation of lateral load, drift, and energy dissipation capacity. The addition of fibers basically may maintain the seismic performance of columns in a slight corrosion level. However, for medium to severe corrosion levels of reinforced concrete columns, the performance is not too much improvement. It could be attributed to significant pitting corrosion occurred on the reinforcing bars leading to a substantial reduction of cross-sectional area. A brittle or sudden failure due to steel fracture on the columns was also observed on the severe corroded level.

*Keywords: Column; Corrosion; Cyclic; Seismic; Polypropylene Fiber*



## 1. Introduction

Nowadays, fiber addition into the concrete mix, namely fiber-reinforced concrete (FRC), has become common in the construction industry, such as in industrial structures as slab-on-grade or containment structures, in transportation infrastructures as pavements or airport runways, and tunnels as shotcrete or precast segmental lining. Many types of fibers are used in concrete, such as steel, synthetic or natural fibers, and micro or macro-fibers. The steel fiber is the most commonly used as fiber addition in concrete, and it has been adopted and regulated in several standards and codes [1, 2], particularly as minimum reinforcement for replacement of conventional reinforcing bars. However, synthetic fibers additions such as polypropylene fibers are still limited to find in the specific guidelines due to limitations in research. FRC offers an enhancement in toughness and ductility compared to plain concrete due to the ability to bridging discrete cracks [3]. In combination with a conventional steel bar, FRC also offers a significant reduction of crack width that could be beneficial to mitigate the structural damage caused by the corrosion of reinforcement to extend the service life.

Corrosion of reinforcement has been known to be one of the most significant causes of structural deterioration of reinforced concrete (RC) structures in corrosive environments. Corrosion may lead to crack or spalling of concrete cover due to corrosion product expansion and may also deteriorate the strength and deformation capacity as results of reduction of reinforcement area and bond deterioration. Several studies about the effect of corrosion on the behavior of RC beams are found in the literature. Among these studies are focused on the effect of reinforcement corrosion on the residual flexural [4, 5, 6] and shear strength [7, 8]. There are also studies about the effect of corrosion on the behavior of RC columns [9] and its seismic performance [10, 11]. However, the experimental study on the seismic behavior and residual strength of corroded FRC members is still limited compared with the experimental work on corroded RC members.

Until now, specific guidelines on design or assessment of the seismic performance of existing fiber reinforced concrete (FRC) structures, especially suffered from corrosion, is still not available due to limited studies [12]. ASCE/SEI 41-13 [13] only emphasis that corrosion of reinforcement should be taken into consideration on structures assessment. Consequently, this may lead to unsafe consideration when the seismic evaluation is conducted on such structures. Therefore, the primary motivation of this study is to have a comprehensive understanding of the seismic behavior and performance of polypropylene fiber-reinforced concrete (PPFRC) columns in various levels of corrosion reinforcement (from slight to severe corrosion) in terms of lateral load resistances, crack patterns and failure modes, hysteretic responses, drift capacities, and energy dissipation capacities. For this purpose, an experimental study is conducted on PPFRC columns that experienced corrosion of longitudinal reinforcements, particularly corrosion that occurred at plastic hinge regions, which are known to play a significant rule in seismic performance of columns.

## 2. Experimental Investigation

The influence of corrosion on the seismic behavior of PPFRC columns was experimentally studied to analyze the seismic performance. The experimental work was conducted at the Structural Engineering Laboratory of Bandung Institute of Technology. All PPFRC columns are loaded with a reversed cyclic lateral load. Before the loading, the PPFRC columns were subjected to the accelerated corrosion process at the plastic hinge regions, except for the control specimens.

### 2.1 Test Specimen Details

The test specimens included five rectangular uncorroded and corroded columns cast with a section dimension of 300 x 300 mm. Two columns acted as control specimens without (RC) or with polypropylene fibers addition (PPFRC) and uncorroded reinforcements. The other three PPFRC columns were subjected to accelerated corrosion for various corrosion levels from slight to severe corrosion damage. For all PPFRC specimens, only 1% of macro-synthetic polypropylene fibers (Fig.1(b)) was added into the concrete mixture. The mechanical properties of polypropylene fibers are presented in Table 3. The column's height was 1500 mm, equal to shear span-to-depth ratio  $a/d$  of 5, and supported with an RC footing at the bottom of the



column. Fig.1(a) shows the specimen's concrete detail and reinforcing bars arrangement. The reinforcement is designed to meet the seismic requirement under ACI 318-14 [2]. The target concrete strength for all test specimens is 35 MPa. For each batch of fresh concrete, six-cylinder specimens of 150 x 300 mm were made for compressive testing at 28 days and testing days. The average compressive strength of the cylinder specimens at testing days are presented in Table 1. Four deformed reinforcing bars of D19 with yield strength 420 MPa and the nominal diameter of 19 mm were used as longitudinal reinforcing bars. The transverse reinforcement of D10, with yield strength 500 MPa and the nominal diameter of 10 mm, were used for all test specimens. The spacing of transverse reinforcement was 100 mm. Table 2 summarizes the mechanical properties of reinforcing bars for all specimens. Corrosion of longitudinal bars is intended to occur at plastic hinge regions near the bottom of columns. Therefore, the longitudinal bars and transverse reinforcements were epoxy-coated to avoid corrosion at the outside hinge regions, including development length regions on RC footings.

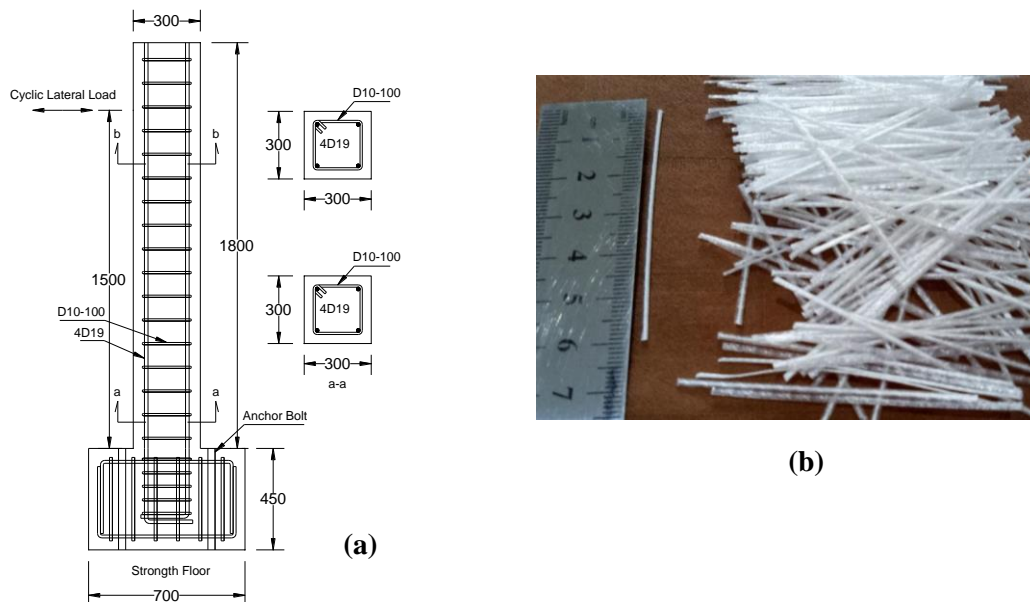


Fig. 1 – Test specimens: (a) reinforcing bars arrangement of columns (Note: all dimension in mm), (b) polypropylene macro-fibers

Table 1 – Test specimens and Corrosion measurements

Specimen	$f'_c$ MPa	Accelerated corrosion time, days	Corrosion level	Concrete Cover crack	
			Mass loss, %	Maximum crack width, mm	Total crack width, mm
RC-C0	35.64	0	0	0	0
FRC-C0	36.24	0	0	0	0
FRC-C1	36.97	8	6.88	0.25	0.7
FRC-C2	37.56	27	12.38	0.5	1.25
FRC-C3	37.35	71	24.96	1.0	2.45



Table 2 – Properties of reinforcing bars

Nominal diameter, mm	$f_y$ , MPa	$f_u$ , MPa	Modulus of elasticity, GPa	Elongation, %
10	500	652	208	16.6
19	420	644	207	20.6

Table 3 – Properties of macro synthetic fiber

Type	Length, mm	Tensile strength, MPa	Young modulus, GPa	Anchorage type
BarChip60	60	640	12	Continuous embossing

## 2.2 Accelerated Corrosion Process

As a natural corrosion process usually takes many years to produce a meaningful corrosion level, the accelerated corrosion process using the electrochemical method was adopted in this study. The accelerated corrosion process was only applied on longitudinal reinforcement at the plastic hinges region as demonstrated in Fig.2. In this study, a constant current density of approximately  $0.5 \text{ mA/cm}^2$  from DC power supply was applied to the reinforcing bars that acted as the anode while the copper plate used as cathodes. As shown in Fig.2, only the plastic hinge region of the column was immersed in the water tank with a 3% sodium chloride (NaCl) solution. Faraday's law was used to estimate the accelerated corrosion time to reach the target of corrosion level. However, in this study, the corrosion loss was determined based on the actual measured data of the experiment. The measurement procedure follows ASTM G1-03 [14] that all reinforcing bars were taken out from the specimens after testing and they were chemically cleaned by 10% of diammonium hydroxide, and then were mechanically cleaned by steel brushes. After that, the weight loss and residual diameter of reinforcing bars along the corroded length were measured to estimate the corrosion levels.

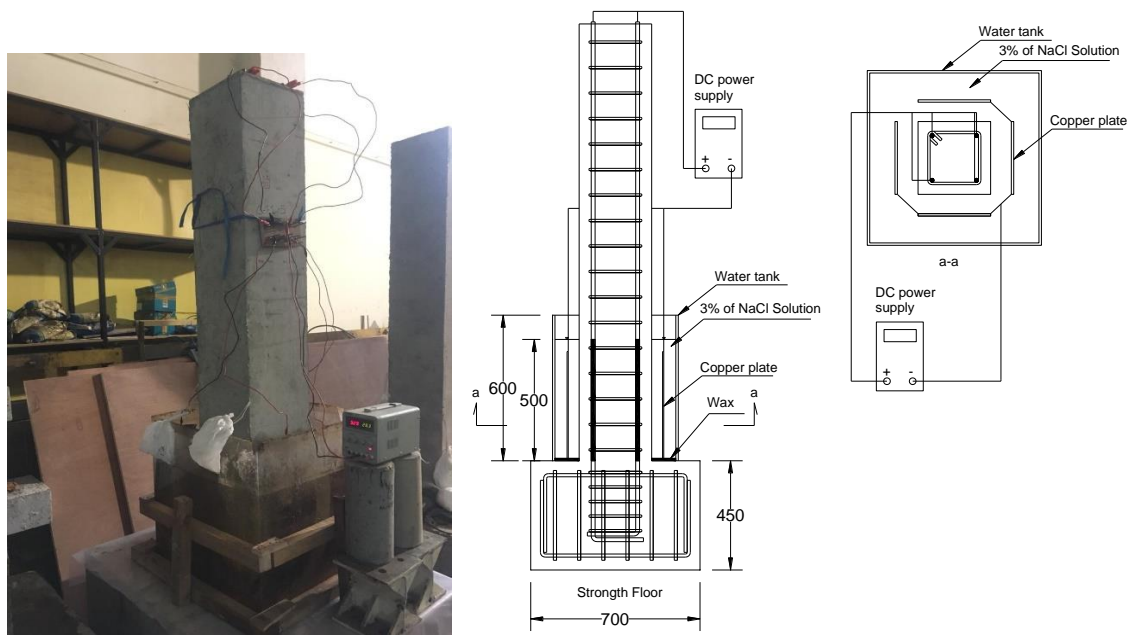


Fig. 2 – Accelerated corrosion setup.



### 2.3 Test Setup and Testing Procedure

Fig.3(a) shows the experimental test setup for test specimens under cyclic loading. In this study, the column specimens were subjected to the reversible horizontal displacement generated from a horizontal actuator with a capacity of 1000 kN to simulate a single curvature bending condition. The cyclic loading history for test specimens is shown in Fig.3(c). Several cycles of lateral displacement were applied, corresponding to the drift ratio from 0.2 to 6%. The drift ratio was determined as the ratio of lateral displacement to the column height, height from the tip of the column to the base of the column. Each drift consists of three cycles of loading, as shown in Fig.3(c). Several linear variable displacement transducers (LVDTs) were installed at several locations to measure the lateral, shear, and flexural deformation, as demonstrated in Fig.3(b). One of them was put at the tip of the column-parallel to the horizontal actuator to measure lateral displacement. No strain gage was put at longitudinal reinforcement due to may damage during accelerated corrosion process, except at transverse reinforcement and uncorroded part of longitudinal reinforcement.

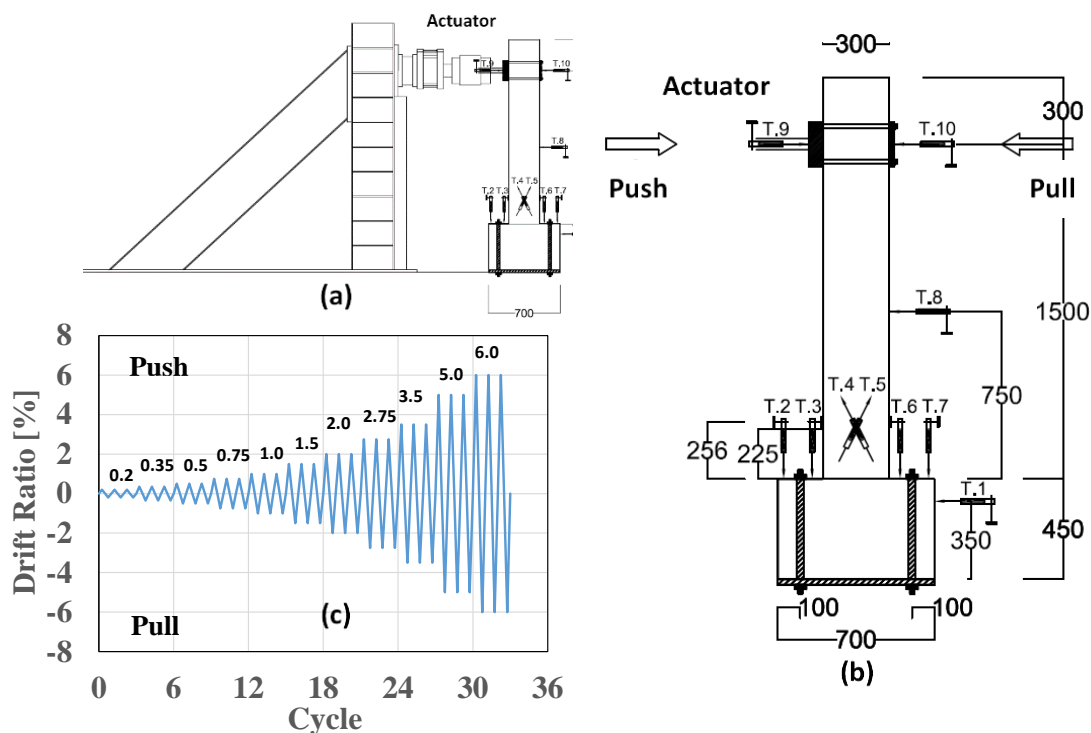


Fig. 3 – (a) Experimental test setup; (b) deformation measurement (c) cyclic loading history

## 3. Experimental Results

This section describes and discusses the experimental results of five uncorroded and corroded RC or PPFRC columns tested with various corrosion levels under lateral cyclic loading.

### 3.1 Load-Displacement Relationships

The load-displacement relationship of all specimens and their envelope is presented in Fig.4(a-e) and Fig.4(f), respectively. As evident in Fig.4(a) and (b), the reference columns FRC-C0 exhibit larger lateral load resistance about 18% compared with the uncorroded RC-C0. It shows a contribution of polypropylene fibers on lateral column capacity that fibers may act as reinforcement or crack bridging as long as fibers anchored to the concrete. The hysteretic response also shows a larger deformability of uncorroded FRC-C0 compares to uncorroded RC-C0. As expected, the hysteretic responses of corroded columns, as shown in Fig.4(a-e), show the lateral-load resistance deterioration and the pinching behavior due to debonding between reinforcement and concrete induced by corrosion.

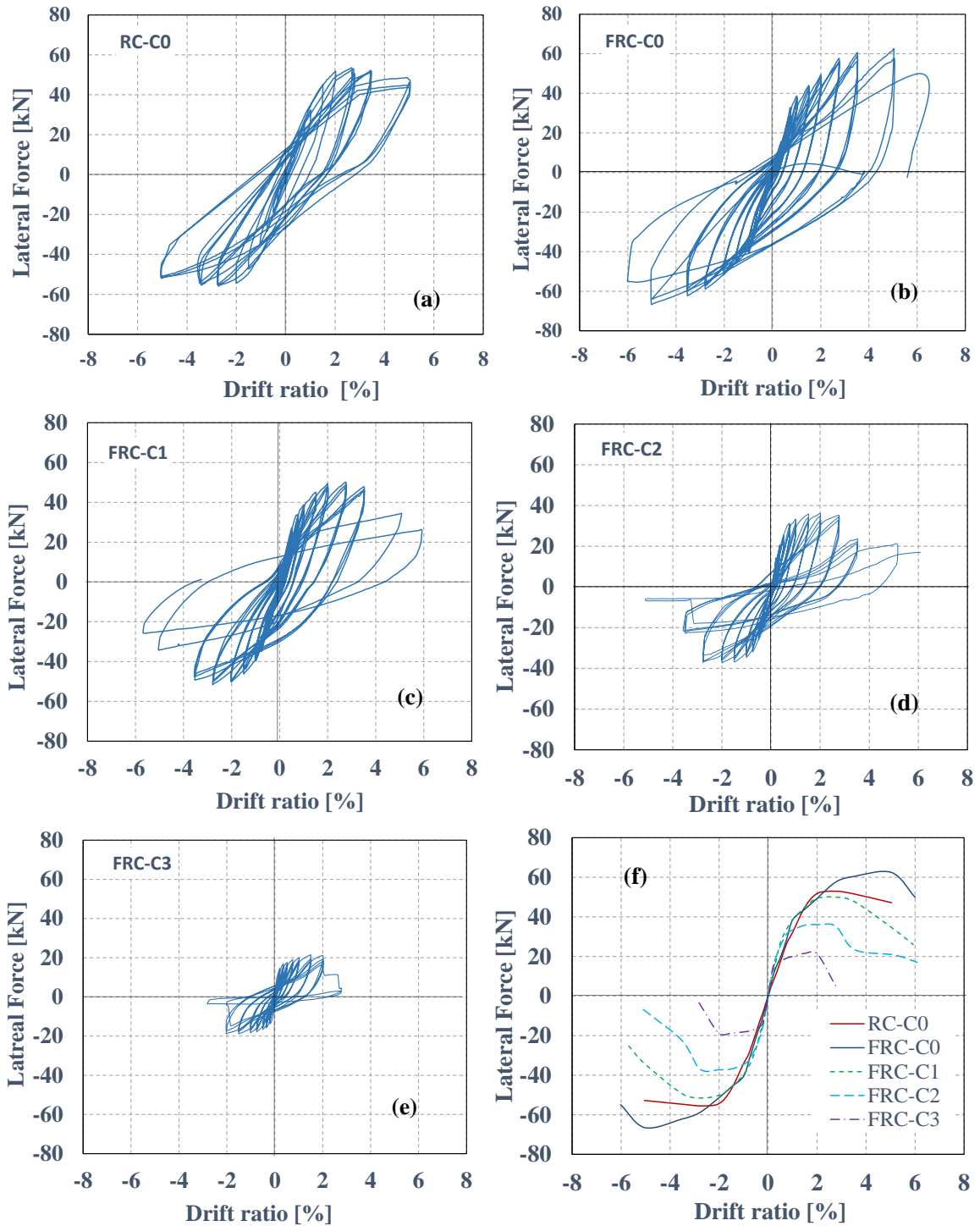


Fig. 4 – (a)-(e) Hysteretic response of test specimens; (f) Backbone curve specimens





### 3.2 Lateral load and drift capacity

Table 4 presents the lateral load capacities of column specimens defined as maximum load resistance. The lateral load capacities decrease with an increase in corrosion levels. Compared to FRC-C0, the reference FRC columns, the lateral load of FRC-C1, C2, and C3 reduced 32%, 43%, and 68%, respectively.

The drift capacity presented in Table 4 is determined in various performance levels as drift ratio at yielding stage, maximum lateral load, and failure stage. In general, drift capacities decreased when corrosion level increased at all performance levels. Regarding the drift capacities at maximum lateral load, a reduction of 53%, 60%, and 70% was observed for FRC-C1, C2 and C3 compared to FRC-C0, respectively. Meanwhile, the drift capacities at failure stage, the reduction of 39%, 49% and 64% were identified for FRC-C1, C2 and C3 compared to FRC-C0, respectively. It is due to the debonding effect and fracture of longitudinal reinforcement induced by corrosion resulting in the significant deterioration of the drift capacities.

### 3.3 Yield displacement and displacement ductility

Theoretically, the yield displacement is defined as the projection to the horizontal axis at the point of intersection between the secant line drawn at the point of 70% of the maximum lateral load, and the horizontal line is drawn corresponding to the maximum lateral load on the hysteretic curve. Table 4 shows the average values of yield displacement from positive and negative loading directions of all test specimens. As indicated, the corrosion significantly affected the yield displacement of specimens. For example, compared to FRC-C0, the yield displacement reduced 65%, 68%, and 85% for corroded for FRC-C1, C2, and C3, respectively. The influence of fibers addition was also identified when compared to uncorroded fibrous concrete FRC-C0 with RC-C0. There is an increase in the yield displacement FRC-C0, about 29% compared to RC-C0. However, for severe corrosion, the influence of fibers addition was insignificant.

Displacement ductility is the ratio of ultimate displacement to yield displacement, as defined previously. As found in the literature [15], ultimate displacement is the measured displacement when the lateral load drops to 85% of the maximum lateral force. Commonly, the displacement ductility is an important parameter to estimate the shear strength of RC columns. The value of displacement ductility is presented in Table 4.

Table 4 – Specimen's comparison with fiber or non-fiber and various corrosion levels

Specimens	Maximum lateral load, kN	Drift ratio, %			Yield displacement, mm	Displacement ductility
		Yielding stage	Max. lateral load	Failure stage		
RC-C0	54.2	1.73	2.75	6.00	25.89	3.48
FRC-C0	64.5	2.43	5.04	6.18	36.38	2.55
FRC-C1	43.6	1.26	2.38	3.78	12.82	3.00
FRC-C2	36.7	0.77	2.01	3.16	11.56	4.10
FRC-C3	20.2	0.37	1.50	2.20	5.48	6.03

### 3.3 Crack patterns and mode of failures

The crack pattern and propagation on the concrete surface of specimens were recorded at every maximum applied displacement at each cyclic loading. Fig. 5 presents the crack pattern at the final stage or end of the test. Two failure modes were identified during the specimen's testing. The first mode is a typical flexural failure as indicated by the horizontal crack perpendicular to the column axis that appeared in the bottom part



of the column. The flexural cracks extended within the plastic hinge regions with the increase of applied load then the flexural shear diagonal cracks were also observed at the last stages of cyclic loading. This failure mode occurred for uncorroded specimens, RC-C0 and FRC-C0, however, compared to fibrous concrete of FRC-C0, the RC-C0 failed with extensive spalling of cover concrete. The corroded FRC-C1, C2, and C3 show less flexural cracks and flexural-shear cracks, the initial longitudinal cracks along longitudinal reinforcements at the plastic hinge region induced by corrosion were also noticeable. The corroded FRC-C2 and C3 failed in flexural shear failure and responded in a more brittle manner. Although the diagonal cracks are not so obviously appeared, the lateral load resistance deteriorated right after the maximum load, and the pinching response was obvious during repeated cyclic loading, as shown in Fig.4. After taking out the reinforcement from the specimens, it is found that the majority of longitudinal reinforcements of FRC-C3 were fracture due to extensive corrosion pitting, causing sudden failure. It was also observed that only non-fiber specimens experience spalling of cover concrete. The FRC specimens did not experience spalling, although they have extensive corrosion. This indicates the advantage of fiber to prevent the disintegration of concrete cover in a higher lateral drift ratio.

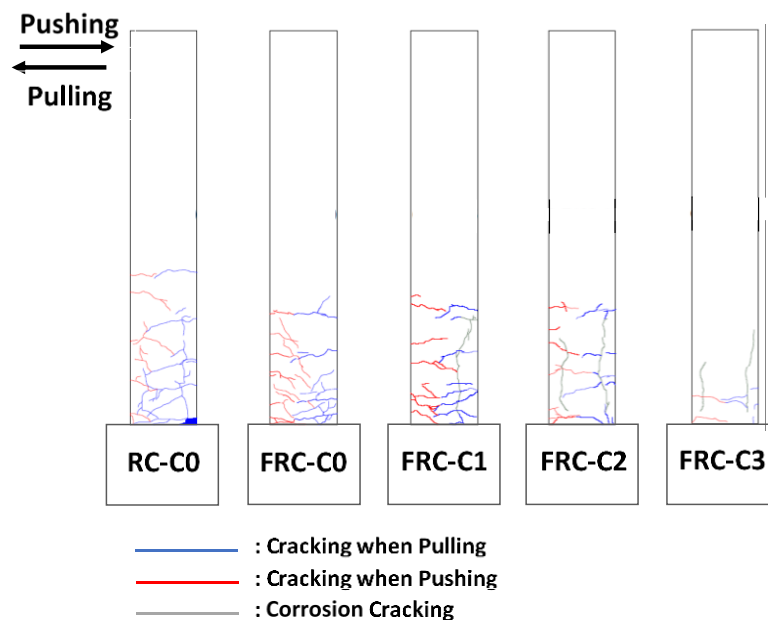


Fig. 5 – Crack patterns of specimens at the final stage.

### 3.4 Energy Dissipation Capacities

The energy dissipation capacity presented in Fig.6 is defined as the area under the hysteretic curve of lateral load and displacement at each cycle. As shown in Fig.6, compared to RC-C0, The FRC-C0 exhibits higher energy dissipation indicated by a well-rounded hysteretic loop, higher lateral load resistance and deformability due to fibers contribution. FRC-C6 (column with light corrosion of 6.8% and RC-C0) was almost similar energy dissipation. This indicates that fiber may maintain the dissipation energy in lower corrosion levels. However, at higher corrosion levels, the energy dissipation deterioration is significant due to extensive pitting corrosion promoting brittle failure, and the influence of fibers is insignificant. As seen in Fig.6, the energy dissipation capacity decrease with an increase of corrosion level and FRC-C3. The highest corrosion level of reinforcing bars is the lowest energy dissipation capacities among other specimens due to reduction of lateral load resistance, drift capacity and pinching effects in the hysteretic curve.



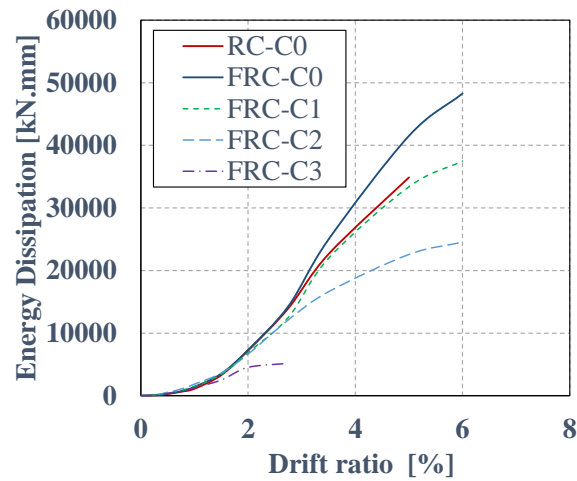


Fig. 6 – Energy dissipation capacities

#### 4. Conclusions

The experimental study on the influence of corrosion on seismic behavior of PPFRC columns under simulated lateral seismic loads is presented. The main parameters investigated in this study are the variation of corrosion levels and polypropylene fiber additions. The following conclusions are drawn:

1. The polypropylene fiber addition into concrete mixture improves the seismic performance in terms of lateral load resistances, drift capacities, and energy dissipation capacities of columns when comparing uncorroded columns with and without fiber addition. Meanwhile, corrosion of reinforcement significantly reduces the lateral load, drift, and energy dissipation capacities. The addition of fibers basically may maintain the seismic performance of columns in a light corrosion level. However, for medium to severe corrosion levels of reinforced concrete columns, the performance is not much improvement. It is attributed to significant pitting corrosion occurred on the reinforcing bars leading to damage concentration and fracture of reinforcing bars.
2. A brittle or sudden failure due to longitudinal bar fracture on the columns was observed on the severely corroded columns due to fracture of longitudinal bars. The fibers addition prevents spalling of concrete covers in which found in non-fibrous columns in higher lateral load or drift.
3. This study results also pointed out the importance of considering the influence of corrosion on the evaluation of the seismic performance of the PPFRC structures particularly on lateral load and drift capacities that may lead to unsafe consideration of the seismic performance level.

#### 5. Acknowledgments

The authors gratefully acknowledge the financial support of the Program of Penelitian, Pengabdian pada Masyarakat dan Inovasi (P3MI) from Institut Teknologi Bandung, Indonesia.

#### 6. References

- [1] CEB-FIP (2012): Model Code 2010: Final Draft, fib Bulletin 65, *Federation Internationale du Beton*, Lausanne, Switzerland.
- [2] ACI 318 Committee (2014): ACI 318-14 Building Code Requirements for Structural Concrete and Commentary, *American Concrete Institute*, USA.



- [3] Bernard, E. S., (2019): Effect of Synthetic Fibers and Aggregate Size on Flexural Crack Widths. *ACI Structural Journal*, **116**(3), 19-26.
- [4] Mangat PS, and Elgarf MS (1999): Flexural Strength of Concrete Beams with Corroding Reinforcement. *ACI Structural Journal*, V. **96**(1), 149-158
- [5] Acosta, AT, Gutierrez, SN.; and Guillen, JT (2007): Residual Flexure Capacity of Corroded Reinforced Concrete Beams. *Engineering Structures*, V. **29**,1145-1152.
- [6] Ou YC, and Nguyen, ND (2016): Influences of Location of Reinforcement Corrosion on Seismic Performance of Corroded Reinforced Concrete Beams. *Engineering Structures*, V. **126**, 210-223.
- [7] Soltani M, Safiey A, and Brennan A (2019): A State-of-the-Art Review of Bending and Shear Behaviors of Corrosion-Damaged Reinforced Concrete Beams. *ACI Structural Journal*, V. **116**(3), 53-64.
- [8] El-Sayed AK, Hussain RR, and Shuraim AB (2016): Influence of Stirrup Corrosion on Shear Strength of Reinforced Concrete Slender Beams. *ACI Structural Journal*, V. **113**(6), 1223-1232.
- [9] Azad AK, Al-Osta MA (2014): Capacity of Corrosion-Damaged Eccentrically Loaded Reinforced Concrete Columns. *ACI Materials Journal*, **111**(6), 711-722.
- [10] Goksu C. and Ilki A., (2016): Seismic Behavior of Reinforced Concrete Columns with Corroded Deformed Reinforcing Bars. *ACI Structural Journal*, V. **113**(5), 1053-1064.
- [11] Vu NS and Li B., (2018): Seismic performance of flexural reinforced concrete columns with corroded reinforcement. *ACI Materials Journal*, **115**(5), 1258-1266.
- [12] Al-Tayyib AH, Al-Zahrani MM, (1990): Corrosion of Steel Reinforcement in Polypropylene Fiber Reinforced Concrete Structures. *ACI Material Journal*, **87**(2), 108-113.
- [13] American Society of Civil Engineers (2014): ASCE/SEI 41-13 Seismic Evaluation and Retrofit of Existing Buildings, *American Society of Civil Engineers*, USA.
- [14] ASTM International (1999): Standard Practice for Preparing, Cleaning, and Evaluation Corrosion Test Specimens (ASTM G1), *ASTM International*.
- [15] ACI 374 Committee 374 (2005): ACI 374.1-05 Acceptance Criteria for Moment Frames Based on Structural testing and Commentary, *American Concrete Institute*, USA.